



Experimental study of the effect of single walled carbon nanotube/water nanofluid on the performance of a two-phase closed thermosyphon

MOHAMMAD CHEHRAZI and BAHAREH KAMYAB MOGHADAS*

Department of Chemical Engineering, Shiraz Branch, Islamic Azad University, Shiraz, Iran

(Received 28 June, revised 26 October, accepted 29 October 2020)

Abstract: Thermosyphons are one of the most efficient heat exchanger apparatus that are used extensively in different industries. One of the most common uses of this device is energy recovery, which is essential due to the energy crisis. Several parameters, such as geometric dimensions, type of working fluid and type of the body, affect the efficiency of a thermosyphon. In this work, the effect of type and concentration of single-walled carbon nanotube nanofluid (SWCNT/water) on the efficiency of heat transfer in a two-phase closed thermosyphon (TPCT) was investigated. For this purpose, a system with a two-phase closed thermosyphon was initially constructed. Then SWCNT/water nanofluids at 0.2, 0.5 and 1 % weight concentration were used as the working fluid in the thermosyphon system. The results of the current experiments showed that the addition of a nanofluid at any weight concentration and an increase in input power increases the performance of the system. In addition, the heat resistance of the TPCT was reduced when the level of SWCNT and input power increased. Hence, for the prepared nanofluid samples, the minimum thermal resistance was obtained at 1 wt. % SWCNT and 120 W. Moreover, the Nusselt number increased with increasing input power and decreased with increasing concentration. In all experiments, all the prepared nanofluid samples had a significantly better thermal performance in comparison with pure water.

Keywords: energy recovery; SWCNT/water-based nanofluid; efficiency; thermal resistance; TPCT.

INTRODUCTION

Apparatuses such as heat pipes are one of the most utilized tools ever known. It could be noted that this system can transmit large quantities of heat at a slight temperature difference in a small cross-section over relatively long dis-

*Corresponding author. E-mail: kamyab@iaushiraz.ac.ir; kamyab_bahareh@yahoo.com
<https://doi.org/10.2298/JSC200628070C>

tances between the hot and cold source, quickly without the need of external power. Perhaps, for this reason, the heat pipe is reminisced as a superconductor.

By investigating nanofluids, it has been shown that these materials, which are a stable and homogenized suspension consisting of a base fluid and additional nanoparticles as an additive, lead to notable enhancement in the thermal performance of this kind of heat exchangers.^{1–4} Additionally, studies showed that compared to fluids without nanoparticles, nanofluids have a significantly higher thermal conductivity.^{5–9}

Kang *et al.*⁶ assayed a nanofluid containing diamond nanoparticles in ethylene glycol as a base fluid. Their result showed an improvement of thermal conductivity of up to 70 % for nanofluid 1 % UDD in ethylene glycol compare to the base fluid. Moreover, Godson *et al.*⁷ demonstrated that Ag/water-based nanofluid leads to an enhancement of 80 % at 0.9 vol. % in thermal conductivity compared to pure water. Zeinali Heris *et al.*^{9–11} investigated the addition of CuO/water-based and Al₂O₃/water-based nanofluid effects on convective heat transfer *via* a roundish tube. Their results led to this fact that by increasing the density of nanofluids, the heat transfer coefficient improves accordingly. Hence Al₂O₃/water-based nanofluids showed better enhancement than CuO/water-based solutions. Noie *et al.*¹² in Ferdowsi Engineering University of Mashhad investigated the heat transfer improvement in a thermosyphon using an Al₂O₃/water-based nanofluid. They investigated the thermal efficiency of a thermosyphon in various volume concentrations of the nanofluid. The results showed that increasing the nanofluid concentration to 3 % by volume concentration would increase the thermal efficiency by up to 14.7 % in comparison with pure water. According to the results of Kang *et al.*,¹³ compared to pure water, the thermal proficiency of an Ag/water-based nanofluid in a heat pipe was comparatively higher. The thermal resistance decreased by 10–80 % compared to DI-water at an input power of 30–60 W. Furthermore, Jia *et al.*¹⁴ studied the heat transfer performance of SiO₂/water-based nanofluids at various concentrations on pulsating heat pipes (PHP), which showed that high concentrations of SiO₂/water reduced the PHP efficiency compared to pure water. This is because of the increase in thermal resistance and evaporator section temperature at high concentrations of SiO₂/water nanofluid. The results of Xu *et al.*¹⁵ showed that hybrid nanofluid 25 % Al₂O₃ + 75 % TiO₂/water-based and the single nanofluid TiO₂/water-based exhibited better thermal performance than deionized water in a TPCT. Another study by Das *et al.*¹⁶ was performed to characterize the thermal performance of a water-based TiO₂ nanofluid with ethylene glycol as a surfactant, and their results evidenced that the use of the nanofluid improved the thermal proficiency of a circular finned thermosyphon by about 20.12 % for 0.30 vol. % TiO₂ nanofluid compared to deionized water as the working fluid.

One of the essential categories of material properties is its thermal properties. The thermal properties of carbon nanotubes are significantly important in various fields of technology, particularly due to the high thermal conductivity of diamond and graphite and the similarities between them. Scientists are interested in studying these properties and found some results in terms of the thermal conductivity of carbon nanotubes in their experimental studies. It has been predicted that carbon nanotubes have a higher thermal conductivity than graphite and diamond at room temperature.¹⁷ Hence, it is necessary to study the performance of carbon nanotubes on the thermal efficiency of thermosyphons because of their thermal properties. Liu *et al.*¹⁸ confirmed the thermal performance improvement and thermal resistance reduction by using CNT/water-based suspension in a weight concentration of 2 % and an operating pressure of 7.4 kPa. Their research showed a 150 % enhancement in heat transfer compared to water at the optimal pressure and concentration. The results of experiments by Choi and Eastman¹⁹ showed that a MWCNT/water-based nanofluid could increase the thermal conductivity more than the base fluid. In addition, Choi *et al.*¹⁹ determined the effective thermal conductivity of MWCNT in oil suspensions. They reported that the measured conductivity enhancements for a 1.0 vol. % nanotubes/oil-based suspension are noticeably greater than those predicted by theoretical models and are about 160 %. Shanbedi *et al.*²⁰ researched multiwalled carbon nanotubes and also suggested the thermal efficiency of a MWCNT/water-based suspension increase, and the Nusselt number and thermal resistance of the thermosyphon diminish on increasing the density of the nanofluid, which led to an increase in the conduction heat transfer by these nanoparticles.

Single-walled carbon nanotubes (SWCNT) are one of the most important types of carbon nanotubes, and the properties vary considerably with different types of SWCNTs. In addition, the results of Pettes and Shi²¹ showed the thermal conductivity of CNTs on the number of walls, and the dependency of the thermal conductivity of CNTs decreases with increasing the number of walls, accordingly. This is attributed to consequential decrease in the concentration of CNTs with increasing number of walls. Despite the advantages of CNTs, some factors; such as poor solubility and instability of aqueous and organic suspensions of CNTs, difficulty in working with them due to their extremely small size, relatively expensive, the current production processes of CNTs, and confined understanding of how CNTs work, has limited their applications. The current work intends to investigate the effects of the addition of (SWCNT) to water as the operating fluid in a two-phase closed thermosyphon, on the Nusselt number, thermal resistance, thermal efficiency, vacuum pressure drop, and evaporator mean temperature. Considering the desirability of the results of experiments and research, the possibility of increasing the efficiency of thermosyphons and pre-

venting the waste of energy in thermal engineering applications will be more than ever possible.

EXPERIMENTAL

In these experiments, single-walled carbon nanotubes with a purity of over 95 %, a length of 5–30 μm , an internal diameter of 0.9–2 nm, and an outer diameter of 1–3 nm were used to prepare a nanofluid that was purchased from VCN Materials Co., Ltd. One of the difficulties of carbon nanotubes is their stability in polar fluids. Arabic gum was used as a surfactant to stabilize the suspension of carbon nanotubes in water. Arabic gum stabilizes carbon nanotubes in polar solvents such as water, due to the creation of non-covalent bondings. Hence, according to reports,²³ in this current study, Arabic gum (AG) was used at a concentration of 0.5 % by weight. Then SWCNT/water nanofluid containing AG was prepared at concentrations of 0.2, 0.5 and 1 % by weight. In order to prepare these concentrations of nanofluid, a balance (AND model GF-1000) with an accuracy of 0.001 g was used. Finally, for further uniformity of the suspension, a sonicator (bath type, operating frequency, and power source of the sonicator are 43 kHz and AC 100–120 V/AC 220–240 V 50/60 Hz, respectively) was used for 5 h. Substances and their weight fractions for prepared nanofluid samples are given in Table I.

Table. I. Substance and weight fraction in different samples of nanofluid

Sample No.	Content of nanoparticles in nanofluid wt. %	Substance for preparation of the nanofluid
1	0.2	SWCNT with purity of 95 %
2	0.5	+ 0.5 wt. % Arabic gum
3	1	

Due to the stability of prepared suspension and the absence of sediment formation in the samples, tests were performed several days after the preparation of the nanofluids. In addition, to evaluate the stability of the nanofluid, transmission electron microscopy (TEM) analysis was provided by the nanofluid manufacturer. After several days from the preparation of the nanofluid until the test, no sediment was observed in the samples. A TEM image of SWCNT/water nanofluid is shown in Fig. 1.



Fig. 1. TEM image of a SWCNT/water sample.

The TPCT set up used in this study is schematically depicted in Fig. 2a, and the constructed apparatus is pictured in Fig. 2b. The primary part of this system is fabricated by a 20 mm×450 mm copper tube with a wall thickness of 1 mm, including the evaporator, adiabatic, and the condenser sections, which are 160, 90 and 200 mm in length, respectively, as

illustrated in Fig. 2a. In addition, the diameter of the casing used in the condenser section is 40 mm. At the outer surface of the copper tube, precisely in the evaporator and condenser sections, four thermocouples (ARVAN model TG-4) were installed to study the process of temperature change in the TPCT system. These K-type thermocouples were positioned at a distance of 5, 10, 15 and 35 cm from the end of the evaporator section, respectively, and were able to measure temperatures in the range of -200 to 1350 °C. Moreover, to observe the temperature changes of the cooling water in the condenser section, two thermometers (CEM DT-131) with an accuracy of 0.1 °C with a temperature range from 0 to 100 °C were used before the inlet and after the outlet of the condenser part. The flow rate of the cooling water was controlled and monitored by a flowmeter (Rotameter LZS-15) with an accuracy of 5 L h⁻¹ in the outlet of the condenser at 15 L h⁻¹. Also, a vacuum pump (Hamer 2RS-5 VE 2100) that makes a vacuum near -85 kPa was used to exhaust the non-condensate gases before testing from the thermosyphon and a pressure gauge to measure the TPCT vacuum pressure. Furthermore, an electrical element with the power of 1000 watts was used to heat the evaporator section. This electrical element was metal and fitted in series with an ammeter (AKB DT-9205A) with an accuracy of 0.01 A and power supply (Variac TDGC2-1KVA) in the circuit. The apparatus was insulated by 2 cm of fiberglass to prevent heat dissipation while considering the thermocouples are adequately protected. Because by contacting the electrical element with these parts, the registered temperatures are unrealistic and higher than expected.

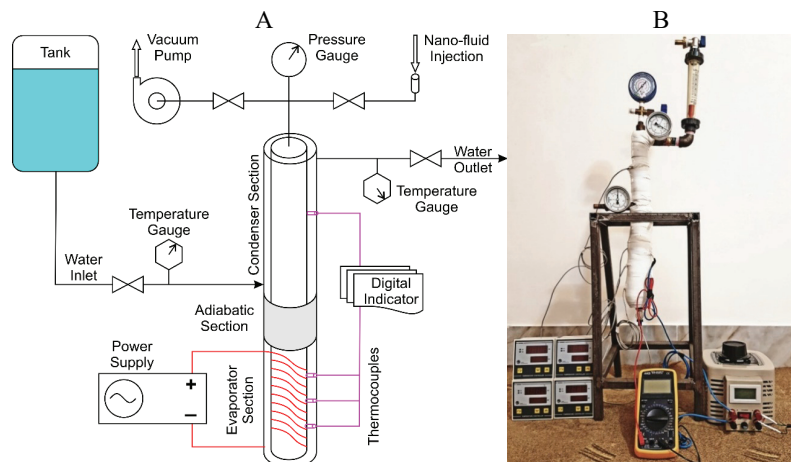


Fig. 2. A – Schematic of TPCT; B – constructed apparatus.

The experimental method was as follows: first, to remove non-condensable gases such as air, the thermosyphon was vacuumed to about -85 kPa by a vacuum pump. The operating fluid of deionized water, with or without the nanoparticles, was then charged into the thermosyphon. In these experiments, a constant filling ratio (FR) of 60 % was used in the system. This ratio is defined as the volume of fluid to the total volume of the evaporator section fraction. The experiment was initially started up with a 30 W input power following up to 30, 45, 60, 90 and finally 120 W afterward with different SWCNT nanofluid concentrations of 0.2, 0.5, and 1.0 wt. % accordingly.

Data processing

The heat transfer rate from the condenser section can be determined as:^{11,23}

$$Q_{\text{out}} = \dot{m}C_p(T_{\text{out}} - T_{\text{in}}) \quad (1)$$

where the variables of \dot{m} , C_p , T_{in} and T_{out} indicate the mass flow rate of the cooling water, the specific heat of the cooling water, inlet temperature, and outlet temperature of the cooling, respectively. The total heat transfer alongside the evaporator section by the electrical element is expressed as follows:^{12,24}

$$Q_{\text{in}} = VI \quad (2)$$

where, V is defined as voltage, and I is defined as electric current of the power supply for various input powers.

Also, an equation is defined to estimate the thermal efficiency of thermosyphon in the following form:¹²

$$\eta = \frac{Q_{\text{out}}}{Q_{\text{in}}} \quad (3)$$

Also, the Nusselt number for a TPCT could be defined as follows:^{25,26}

$$Nu = \frac{Q_{\text{net,conv}}}{Q_{\text{net,cond}}} \quad (4)$$

where $Q_{\text{net,conv}}$ indicates the amount of net convective heat transfer and $Q_{\text{net,cond}}$ indicates the net conductive heat transfer amount. The amount of the net convective heat transfer is obtained by Eq. (1), while the net conductive heat transfer amount is determined as:²⁴

$$Q_{\text{net,cond}} = \pi r^2 K_{\text{nf}} \frac{\Delta T}{L} \quad (5)$$

where r is the radius, and L is the length of the TPCT, K_{nf} is the thermal conductivity coefficient of the nanofluid, and ΔT is the temperature difference between the condenser and the evaporator section.

Therefore, according to these definitions, the Nusselt number of TPCT is calculated from:

$$Nu = \frac{\dot{m}C_p(T_{\text{out}} - T_{\text{in}})}{\pi r^2 K_{\text{nf}} \Delta T / L} \quad (6)$$

In Eq. (6), only K_{nf} is unknown. Various models have been presented for the estimation of the nanofluid thermal conductivity. However, all of these models are valid only for compounds containing spherical or oval-shaped particles with a small axis ratio. While carbon nanotubes can be considered as oval-shaped nanoparticles with a large axial ratios. Moreover, the existing models cannot explain the effect of CNT spatial distribution on the coefficient of thermal conductivity. Accordingly, Xue²⁷ presented an equation based on the Maxwell model to calculate the thermal conductivity of CNT containing nanofluids, including the effect of a large axis ratio and spatial distribution of carbon nanotubes. The, Xue equation is defined to estimate the thermal conductivity coefficient:

$$K_{\text{nf}} = \frac{(1-\nu) + 2\nu\alpha \ln(\gamma)}{(1-\nu) + 2\nu\beta \ln(\gamma)} K_{\text{bf}} \quad (7)$$

where

$$\alpha = \frac{K_{\text{CNT}}}{K_{\text{CNT}} - K_{\text{bf}}}, \beta = \frac{K_{\text{bf}}}{K_{\text{CNT}} - K_{\text{bf}}}, \gamma = \frac{K_{\text{bf}} + K_{\text{CNT}}}{2K_{\text{bf}}}$$

and ν describes the volume fraction of the nanotubes of the nanofluid. Therefore, considering the volume fraction of carbon nanotubes used in this study were 0.095, 0.238 and 0.476 for nanofluid with a concentration of 0.2, 0.5 and 1 % by weight, respectively. While, K_{bf} , K_{nf} , and K_{CNT} are the thermal conductivity of pure water, nanofluid, and carbon nanotubes, respectively.

The thermal resistance (R_{th}) for the TPCT was obtained from:^{18,28}

$$R_{\text{th}} = \frac{T_e - T_c}{Q} \quad (8)$$

where, T_e and T_c are defined as the temperatures of the evaporator and condenser section, respectively, and Q indicates the amount of the heat transferred from the condenser section.

In this study, the uncertainty could be estimated by Holman Correlation as follows:²⁹

$$\text{Max } E_\eta = \pm \left\{ (E_{Q_{\text{out}}})^2 + (-E_{Q_{\text{in}}})^2 \right\}^{0.5} \quad (9)$$

$$\text{Max } E_{Q_{\text{out}}} = \pm \left\{ (E_m)^2 + (E_{C_p})^2 + (E_{(T_{\text{out}} - T_{\text{in}})})^2 \right\}^{0.5} \quad (10)$$

$$\text{Max } E_{Q_{\text{in}}} = \pm \left\{ (E_V)^2 + (E_I)^2 \right\}^{0.5} \quad (11)$$

Since the maximum precision of the voltmeter, ammeter and thermometer is 1 V, 0.01 A and 0.1 °C, respectively, the maximum uncertainties in the obtained thermal efficiency is 3.5 %.

RESULTS AND DISCUSSION

The thermal efficiency results of the two-phase closed thermosyphon (TPCT) were observed. The factors of the thermal efficiency, thermal resistance, and the Nusselt number are investigated under different operating conditions, as the essential factors affecting the thermal performance of a closed thermosyphon. The effect of parameters such as sample type and nanofluid concentration under various input powers on the thermal performances of two-phase closed thermosyphons (TPCT) were investigated, and the respective diagrams with complete discussion are given. In addition, the temperature distribution on the external surface of the core cylinder of the TPCT, which can be a good indication of the thermal resistance and the vacuum pressure drop in the thermosyphon, are discussed.

In this research, experiment operations were performed at 30, 45, 60, 90 and 120 W input powers in accordance with three weight (volume) concentrations of the SWCNT/water suspension (nanofluid) of 0.2 % (0.095 %), 0.5 % (0.238 %), and 1 % (0.476 %) CNT concentrations. A 3D and linear diagram for the variability of thermal efficiency with a constant input power at a different weight fraction of nanoparticles for the five diverse input powers used in this study are shown in Fig. 3. Thermal efficiency increases with increasing input power and weight fraction of nanoparticles. This enhancement of thermal efficiency depends

on the heat transfer behavior of the nanostructure. Nanoparticles, with their Brownian motion, result in a noticeable rise in the rate of the heat transfer between the fluid and nanotube wall.¹¹ Therefore, as the nanofluid weight fraction increases, the TPCT thermal efficiency also increases, because the addition of nanostructure into the base fluid enhances the particle collisions in the TPCT. As shown in Fig. 3, the thermal efficiency in the lower concentrations is significantly increased, but at higher concentrations, the increase is less. For example, in the range of 30 to 45 W for input power at a concentration of 0.2 wt. %, the thermal efficiency of the TPCT was increased by about 10 %. According to Fig. 3, it was observed that the nanofluid sample with a concentration of 1 wt. % of SWCNT obtained the highest efficiencies at all input powers, and the maximum efficiency of about 89 % was reported for an input power of 120 W. In this study, for an input power of 120.75 W (voltage = 75 V, $I = 1.61$ A) and concentration of 1 wt. %, the temperature of the inlet (T_{in}) and outlet (T_{out}) cooling water reached 19 and 25.1 °C, respectively. According to Eq. (1) and at a mass flow rate of cooling water of $0.00415 \text{ kg s}^{-1}$, the Q_{out} obtained about 107.09 W. By substituting the values of Q_{out} and Q_{in} in Eq. (3), the obtained thermal efficiency of thermosyphon was about 0.89.

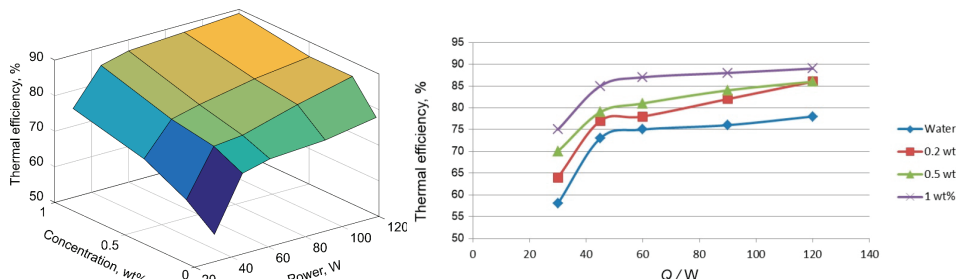


Fig. 3. The TPCT thermal efficiency vs. input power and concentration of nanofluid.

The dimensionless Nusselt number in a thermosyphon represents the ratio of the heat transferred through displacement to that transferred through conduction, which is obtained from Eq. (6). In this study, the variation of the Nusselt number under different concentrations of carbon nanotubes and various input power is shown in Fig. 4.

According to Fig. 4, the Nusselt number decreases with increasing concentration of carbon nanotubes in the nanofluid. For example, a nanofluid with 0.2 wt.% of CNT, the Nusselt number at 30 W is about 145.19, while at a concentration of 0.5 and 1.0 wt. % of CNT, these values are about 70.22 and 30.26 at the same input power, respectively. According to Eq. (7), with increasing concentration of carbon nanotubes, the coefficient of thermal conductivity for the nanofluid (K_{nf}) increases and considering the definition of the Nusselt number in

Eq. (6) by increasing the denominator, the Nusselt number decreases consequently, which represents the increase in heat transfer through the conduction mechanism.

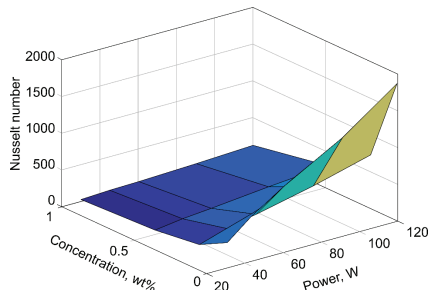


Fig. 4. The thermosyphon Nusselt number versus input power and concentration of nanofluid.

Increasing in the input power, the thermal resistance of the TPCT decreases, whereas, according to Eq. (8), the thermal resistance has an inverse relation to power. However, the reduction of thermal resistance at lower power is more than at a higher power. In addition, by increasing the concentration of SWCNT in the nanofluid, the resistance against the thermal proficiency of the thermosyphon is reduced. For example, at an input power of 30 W, the highest and the lowest thermal resistance are related to water ($2.34 \text{ }^{\circ}\text{C W}^{-1}$) and nanofluid 1.0 wt. % of CNT ($1.71 \text{ }^{\circ}\text{C W}^{-1}$), respectively. In this study, at an input power of 30.24 W (voltage = 36 V, $I = 0.84 \text{ A}$), the average evaporator temperature, condenser temperature, and temperature difference of condenser section obtained about 62.9, 21.8 and $1 \text{ }^{\circ}\text{C}$ for water and 61.2, 22.3 and $1.3 \text{ }^{\circ}\text{C}$ for nanofluid 1.0 wt. %, respectively. The variation of thermal resistance against the input power of the TPCT is plotted in Fig. 5.

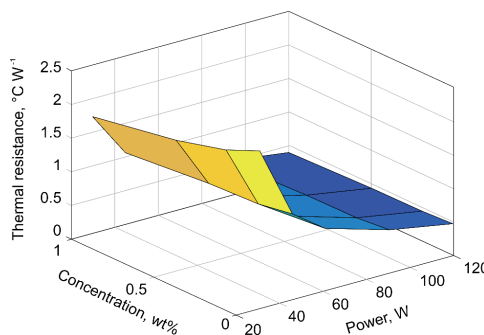


Fig. 5. The thermal resistance of TPCT (in the condenser section) vs. input power and concentration of the nanofluid.

Bubble formation at the liquid–solid interface of the TCPT is considered to be the primary cause of the thermal resistance. The larger size of these bubbles leads to the creation of higher amounts of thermal resistance, which interferes with the heat transfer from the solid surface to the fluid. In the presence of nano-

particles dispersed in the fluid, the vapor bubbles will explode at the first moments of formation. Therefore, much smaller vapor bubbles should be did not contain any nanoparticles, which consequently reduces the thermal resistance of the TPCT.^{29–33}

Variations in the vacuum pressure drop of the operating fluid are shown in Fig. 6 for each test. It was observed that with increasing nanofluid concentration, the vacuum pressure drop increased, because at higher pressure, the boiling point of the fluid was even higher, and the thermal proficiency of thermosyphon was reduced. In this study, the maximum vacuum pressure drop was obtained for a SWCNT concentration of 1 wt. %. Although the nanofluid had the highest thermal efficiency, it also had the biggest top vacuum pressure drop.

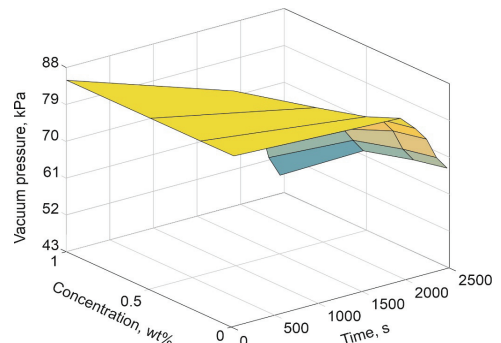


Fig. 6. Vacuum pressure drop vs. experiment time and concentration of the nanofluid.

The average temperature of the evaporator section against various input power with various concentrations of SWCNT is plotted in Fig. 7. According to the results of experiments, one could expect the power of 90 and 120 W as the density of nanofluid rises, while the evaporator section average temperature decreases too. For example, at an input power of 45 W, the evaporator section is at average temperature for water, whereas the nanofluid of 0.2, 0.5, and 1 wt. % heats to about 63.9, 63.8, 63.7 and 62.9 °C, respectively. According to Eq. (8), the thermal resistance is directly related to the variations of temperature between the evaporator and condenser section. Hence, with a reduction of the average temperature of the evaporator section, the temperature difference between the evaporator and condenser section evidently decreased, which represents a reduction of the thermal resistance in the TPCT. The thermal resistance of the thermosyphon core surface, the evaporation and condensation process thermal resistances, and the two-phased flow resistance alongside the length of the TPCT form the overall thermal resistance of a thermosyphon totally in between the evaporation core and the condenser section.²⁰ The surface properties of the interior surfaces of the thermosyphon, such as wettability and roughness, effect the bubbles formation and, consequently, the thermal resistance in the evaporator and condenser section. Using nanofluids, by increasing thermal conductivity and

density of the liquid and decreasing the diameter of the released bubbles, leads to reduced thermal resistance and temperature in the evaporator section.^{12,24,29,30} On the other hand, the reason of increasing temperature in the evaporator section at high input power (90 and 120 W) and low concentrations (0.2 and 0.5 wt. %) could be related to an increase in the number of bubbles at high input power and the inability of the nanofluid to explode these bubbles at low concentrations.

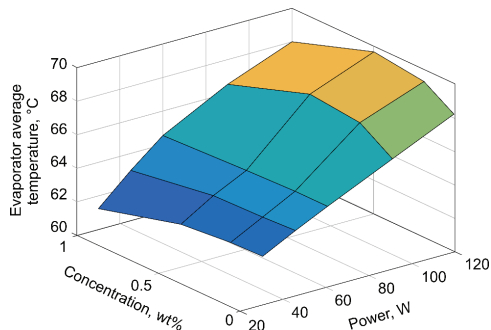


Fig. 7. The average temperature distribution of the evaporator section of the TPCT vs. input power and concentration of the nanofluid.

A comparison between the performance of MWCNT & SWCNT in the TPCT

The research carried out on the performance of MWCNT/water nanofluid as the operating fluid in a TPCT²⁰ indicates that at a concentration of 1 wt. % ($R = 0.43$) and 90 W input power, which has the highest thermal efficiency, the thermal resistance in condenser section decreased to about 12.24 % compared to the water as the base fluid ($R = 0.49$). While this reduction for SWCNT/water nanofluid at a concentration of 1 wt. % ($R = 0.52$) and the same input power compared to water ($R = 0.63$) is about 17.46 %. In addition, improvement in the thermal efficiency of the thermosyphon at an input power of 90 W is about 12.19 % after applying MWCNT/water nanofluid at a concentration of 1 wt. % ($\eta = 0.8944$) compared to pure water ($\eta = 0.7972$). While this improvement in thermal efficiency for SWCNT/water nanofluid at a concentration of 1 wt. % ($\eta = 0.88$) and the same input power is about 15.78 % compared to water ($\eta = 0.76$). Moreover, to achieve steady-state conditions and a thermal efficiency of 89 % needs about 5200 s when using MWCNT/water nanofluid, while the time for SWCNT/water nanofluid to achieve to this thermal efficiency is about 2215 s.

CONCLUSIONS

In this research, the experiments were carried out with a TPCT initiated by input powers of 30, 45, 60, 90 and 120 W along with SWCNT concentrations of 0.2, 0.5 and 1.0 wt. % in the operating nanofluid. The purpose of the current research was to explore the effect of the addition of SWCNT nanoparticles into the operating fluid of a TPCT on the thermal efficiency and its leading parameters, such as vacuum pressure drops, the average temperature of the TCPT

evaporator, Nusselt number, and the thermal resistance of the apparatus. In this section, the most relevant results of this research are mentioned. The results show that SWCNT/water nanofluids at all concentrations lead to improved thermal proficiency of a TPCT. By increasing the density of the nanofluid and electrical power, the thermal efficiency of the TCPT also increases, the improvement in thermal efficiency being more significant at lower input power. Additionally, by increasing the concentration of SWCNT in the operating nanofluid, the Nusselt number of the TPCT decreases, which, together with input power increase, will lead to a reduction in the thermal resistance. The minimum thermal resistance will occur at a concentration of 1 wt. %. Moreover, by condensing the nanofluid, the vacuum pressure drop in the TPCT increases. Also, by increasing the concentration of nanofluids at all amounts of input power, the average temperature of the evaporator section is reduced (except 90 and 120 W at a concentration of 0.2 and 0.5 wt. %), which is confirmed by a reduction in the thermal resistance at the evaporator section. Furthermore, on comparing the performance of the MWCNT/water and SWCNT/water nanofluids on a TPCT, it was observed that SWCNT nanofluid has higher thermal efficiency that leads to a greater reduction in thermal resistance at a TPCT.

NOMENCLATURE

C_p	water specific heat, $\text{J kg}^{-1} \text{K}^{-1}$
I	current, A
K_{bf}	base fluid thermal conductivity, $\text{W m}^{-1} \text{K}^{-1}$
K_{CNT}	carbon nanotube thermal conductivity, $\text{W m}^{-1} \text{K}^{-1}$
K_{nf}	nanofluid thermal conductivity, $\text{W m}^{-1} \text{K}^{-1}$
L	length of evaporator section, m
\dot{m}	water mass per unit time, kg s^{-1}
Nu	Nusselt number
Q_{in}	input heat transfer by evaporation, W
$Q_{net, cond}$	net conductive heat transfer, W
Q_{out}	output heat transfer by condensation, W
r	radius, m
R_{th}	thermal resistance, K W^{-1} or $^{\circ}\text{C W}^{-1}$
T_e	evaporator temp, $^{\circ}\text{C}$
T_c	condenser temp, $^{\circ}\text{C}$
T_i	inlet temp of cooling water, K
T_o	outlet temp of cooling water, K
V	voltage, V
ΔT	temperature difference ($T_e - T_c$), $^{\circ}\text{C}$
$Q_{net,conv}$	net convective heat transfer, W
<i>Greek letters</i>	
η	efficiency of two-phase closed thermosiphon
ν	volume concentration (%)

ИЗВОД

ЕКСПЕРИМЕНТАЛНО ИСПИТИВАЊЕ УГЉЕНИЧНИХ НАНОЦЕВИ СА
ЈЕДНОСТРУКИМ ЗИДОМ/ЕФЕКАТ ВОДЕНОГ НАНОФЛУИДА НА ПЕРФОРМАНСЕ
ДВОФАЗНОГ ЗАТВОРЕНОГ ТЕРМОСИФОНА

МОХАММАД СХЕХРАЗИ и ВАХАРЕХ КАМЯБ МОГХАДАС

Department of Chemical Engineering, Shiraz Branch, Islamic Azad University, Shiraz, Iran

Термосифони су међу најефикаснијим апаратима за размену топлоте који се користе у различитим индустријама. Једна од најчешћих употреба ових уређаја је ренегација енергије, што је изузетно битно, с обзиром на енергетску кризу. Неколико параметара, као што су геометријске димензије, тип радног флуида, тип тела термосифона, утиче на ефикасност термосифона. У овом експерименту испитиван је утицај типа и концентрације воденог нанофлуда са угљеничним наноцевима са једноструким зидом (*single-walled carbon nanotube nanofluid – SWCNT*) на ефикасност преноса топлоте у двофазном затвореном термосифону (*two-phase closed thermosyphon*). За ову сврху, најпре је конструисан двофазни затворени термосифон. Затим су водени SWCTN нанофлуди са тежинским концентрацијама 0,2; 0,5 и 1 % коришћени као радни флуид у термосифонском систему. Резултати експеримената су показали да додатак нанофлуда било које концентрације и повећање улазне снаге побољшавају перформанце система. Такође, топлотни отпор двофазног затвореног термосифона опада са повећањем нивоа SWCNT и улазне снаге. Тако, за припремљене узорке нанофлуда, најмања вредност топлотног отпора је добијена за 1 % SWCNT и 120 W. Такође, нуселтов број расте са повећањем улазне снаге и смањује се са повећањем концентрације. У свим експериментима, сви припремљени узорци нанонфлуда су имали значајно боље топлотне перформансе у поређењу са чистом водом.

(Примљено 28. јуна, ревидирано 26. октобра, прихваћено 29. октобра 2020)

REFERENCES

1. M. Ramezanizadeh, M. A. Nazari, M. H. Ahmadi, E. Açıkkalp, *J. Mol. Liq.* **272** (2018) 395 (<https://doi.org/10.1016/j.molliq.2018.09.101>)
2. H. Karami, S. Papari-Zare, M. Shanbedi, H. Eshghi, A. Dashtbozorg, A. Akbari, C. B. Teng, *Int. Commun. Heat Mass* **108** (2019) 104302 (<https://doi.org/10.1016/j.icheatmasstransfer.2019.104302>)
3. A. O. Borode, N.A. Ahmed, P. A. Olubambi, *Nano-Struct. Nano-Objects* **20** (2019) 100394 (<https://doi.org/10.1016/j.nanoso.2019.100394>)
4. E. Živković, S. Kabelac, S. Šerbanović, *J. Serb. Chem. Soc.* **74** (2009) 427 (<https://doi.org/10.2298/JSC0904427Z>)
5. S. U. Choi, J. A. Eastman, *International Mechanical Engineering Congress and Exposition*, in *Enhancing Thermal Conductivity of Fluids with Nanoparticles*, San Francisco, CA, 1995, p. 12
6. H. U. Kang, S. H. Kim, J. M. Oh, *Exp. Heat Transf.* **19** (2006) 181 (<https://doi.org/10.1080/08916150600619281>)
7. L. Godson, B. Raja, D. M. Lal, S. Wongwises, *Exp. Heat Transf.* **23** (2010) 317 (<https://doi.org/10.1080/08916150903564796>)
8. H. R. Goshayeshi, M. R. Safaei, M. Goodarzi, M. Dahari, *Powder Technol.* **301** (2016) 1218 (<https://doi.org/10.1016/j.powtec.2016.08.007>)
9. S. Zeinali Heris, M. N. Esfahani, G. Etemad, *J. Enhanc. Heat Transf.* **13** (2006) 279 (<https://doi.org/10.1615/JEnhHeatTransf.v13.i4.10>)

10. S. Zeinali Heris, G. Etemad, M. Nasr Esfahany, *Int. Commun. Heat Mass* **33** (2006) 529 (<https://doi.org/10.1016/j.icheatmasstransfer.2006.01.005>)
11. S. Zeinali Heris, M. Nasr Esfahany, G. Etemad, *Int. J. Heat Fluid Flow* **28** (2007) 203 (<https://doi.org/10.1016/j.ijheatfluidflow.2006.05.001>)
12. S. H. Noie, S. Zeinali Heris, M. Kahani, S. M. Nowee, *Int. J. Heat Fluid Flow* **30** (2009) 700 (<https://doi.org/10.1016/j.ijheatfluidflow.2009.03.001>)
13. S. W. Kang, W. C. Wei, S. H. Tsai, S. Y. Yang, *Appl. Therm. Eng.* **26** (2006) 2377 (<https://doi.org/10.1016/j.applthermaleng.2006.02.020>)
14. H. J. Jia, L. Jia, Z. Tau, *J. Therm. Sci.* **22** (2013) 484 (<https://doi.org/10.1021/ma302119t>)
15. Q. Xu, L. Liu, J. Feng, L. Qiao, Ch. Yu, W. Shi, Ch. Ding, Y. Zang, Ch. Chang, Y. Xiong, Y. Ding, *Int. J. Heat Mass Transf.* **149** (2020) 119189 (<https://doi.org/10.1007/s11630-020-1273-7>)
16. S. Das, A. Giri, S. Samanta, *Energy Source, A* (2020) 1 (<https://doi.org/10.1080/15567036.2020.1727998>)
17. S. Berber, Y. K. Kwon, D. Tomanek, *Phys. Rev. Lett.* **84** (2000) 4613 (<https://doi.org/10.1103/PhysRevLett.84.4613>)
18. Z. H. Liu, X. F. Yang, G. S. Wang, G. L. Guo, *Int. J. Heat Mass Transf.* **53** (2010) 1914 (<https://doi.org/10.1016/j.ijheatmasstransfer.2009.12.065>)
19. S. U. Choi, Z. G. Zhang, W. Yu, F. E. Lockwood, E. A. Grulke, *Appl. Phys. Lett.* **79** (2001) 2252 (<https://doi.org/10.1063/1.1408272>)
20. M. Shanbedi, S. Zeinali Heris, M. Baniadam, A. Amiri, *Exp. Heat Transf.* **26** (2013) 26 (<https://doi.org/10.1080/08916152.2011.631078>)
21. M. T. Pettes, L. Shi, *Adv. Funct. Mater.* **19** (2009) 3918 (<https://doi.org/10.1002/adfm.200900932>)
22. D. Wen, Y. Ding, *J. Thermophys. Heat Transf.* **18** (2004) 481 (<https://doi.org/10.2514/1.9934>)
23. Y. Yang, E. A. Grulke, Z. G. Zhang, G. Wu, *J. Appl. Phys.* **99** (2006) 114307. (<https://doi.org/10.1063/1.2193161>)
24. S. H. Noie, *Appl. Thermal Eng.* **25** (2005) 495 (<https://doi.org/10.1016/j.applthermaleng.2004.06.019>)
25. S. Maki, T. Tagawa, H. Ozoe, *J. Heat Transf.* **124** (2002) 667 (<https://doi.org/10.1115/1.1482082>)
26. H. Salehi, S. Zeinali Heris, S. H. Noie, *J. Enhanced Heat Transf.* **18** (2011) 261 (<https://doi.org/10.1615/JEnhHeatTransf.v18.i3.70>)
27. Q. Z. Xue, *Physica B* **368** (2005) 302 (<https://doi.org/10.1016/j.physb.2005.07.024>)
28. S. Khandekar, Y. M. Joshi, B. Mehta, *Int. J. Ther. Sci.* **47** (2008) 659 (<https://doi.org/10.1016/j.ijthermalsci.2007.06.005>)
29. J. D. Holman, *Experimental Methods for Engineers*, 5th ed., Ch. 3, McGraw-Hill, New York, 1989
30. H. Sardarabadi, S. Z. Heris, A. Ahmadpour, M. Passandideh-Fard, *Energy Conv. Manage.* **188** (2019) 321 (<https://doi.org/10.1016/j.enconman.2019.03.070>)
31. M. M. Sarafraz, I. Tlili, Z. Tian, M. Bakouri, M. R. Safaei, *Physica A* **534** (2019) 122146 (<https://doi.org/10.1016/j.physa.2019.122146>)
32. C. Li, Z. Wang, P. Wang, Y. Peles, N. Koratkar, G. P. Peterson, *Small* **4** (2008) 1084 (<https://doi.org/10.1002/smll.200700991>)
33. S. J. Kim, I. C. Bang, J. Buongiorno, L. W. Hu, *Int. J. Heat Mass Transf.* **50** (2007) 4105 (<https://doi.org/10.1016/j.ijheatmasstransfer.2007.02.002>).